Estuaries and Coasts
https://doi.org/10.1007/s12237-024-01422-y

Projecting Mangrove Forest Resilience to Sea-Level Rise on a Pacific Island: Species Dynamics and Ecological Thresholds

Kevin J. Buffington[1] · Joel A. Carr[2] · Rich A. MacKenzie[3] · Maybeleen Apwong[4] · Ken W. Krauss[5] · Karen M. Thorne[1]

Received: 27 September 2023 / Revised: 12 August 2024 / Accepted: 14 August 2024

Abstract

Mangroves can increase their elevation relative to tidal flooding through biogeomorphic feedbacks but can submerge if rates of sea-level rise are too great. There is an urgent need to understand the vulnerability of mangroves to sea-level rise so local communities and resource managers can implement and prioritize actions. The need is especially pressing for small islands, which have been identified as an area of concern by the IPCC. We developed a generalizable modeling framework for tidal wetlands (WARMER-3) that accounts for species interactions and the belowground processes that dictate soil elevation building relative to sea levels. The model was calibrated with extensive field datasets, including accretion rates derived from 29 soil cores, over 300 forest inventory plots, water level, and elevation. The model included five mangrove tree species and was applied across seven regions around the Pacific Island of Pohnpei, Federated States of Micronesia, where mangrove forest is a critical ecosystem that supports subsistence living for local communities. We explored mangrove resilience and carbon accumulation under six sea-level rise scenarios. We also conducted an analysis to determine the sea-level rise rate threshold above which mangroves would be lost. The results suggest that Pohnpei mangroves can build their elevations relative to low and moderate rates of sea-level rise to prevent submergence, with limited loss of mangrove area through 2150. Under higher sea-level rise rates, however, forest elevation decreased substantially relative to mean sea level and there was extensive loss of mangrove area by that year. Regarding mangrove community composition, for all sea-level rise scenarios, the model predicted a change to increasing relative abundance of flood tolerant species and decreasing relative abundance of high-elevation species, which started to being realized by 2100. Variation in sediment supply, water levels, and elevation capital led to differential vulnerability around the island. We identified a threshold for Pohnpei mangroves where if local sea-level rise rates exceed 7.8 ± 2.2 mm/year they are projected to eventually submerge and be lost. Our modeling framework is novel by addressing both species interactions and critical belowground processes to better understand potential tidal ecosystem responses to sea-level rise.

Keywords Modeling · Vulnerability · Coastal wetlands · Climate change · Monte Carlo

Key Points

- Mangrove forests were shown to be resilient to low and moderate sea-level rise projections through 2150, but extensive loss would occur under high sea-level rise projections.
- Forest species composition is projected to change under all sea-level rise scenarios with a shift to more flood tolerant species.
- Modeling suggests a threshold sea-level rise rate of 7.8 mm/year for the mangrove forest of the island of Pohnpei, beyond which conversion to subtidal habitats is likely.

Introduction

Management and conservation in the context of a rapidly changing climate requires an understanding of ecological thresholds, tipping points, and regime shifts (Andersen et al. 2009). This is particularly true for the coastal zone, which is already dynamic in nature. At the interface between marine

✉ Kevin J. Buffington
kbuffington@usgs.gov

[1] Western Ecological Research Center, U.S. Geological Survey, Davis, CA, USA

[2] Eastern Ecological Science Center, U.S. Geological Survey, Laurel, MD, USA

[3] Institute of Pacific Islands Forestry, USDA Forest Service, Hilo, HI, USA

[4] University of Hawaii at Hilo, Hilo, HI, USA

[5] Wetland and Aquatic Research Center, U.S. Geological Survey, Lafayette, LA, USA

Published online: 04 October 2024

and terrestrial environments along tropical and subtropical latitudes, mangrove forests are exposed to tidal flooding, storms, and accelerating sea-level rise (SLR), which is projected by global models as a consequence of climate change (Fox-Kemper et al. 2021). Mangrove forests exist in a narrow ecological niche, tolerant of regular inundation by saline water but outcompeted by upland species above the tidal zone. These tidal wetlands are sensitive to the rate of SLR, but may be able to persist through a combination of accretion and inland migration (Kirwan et al. 2016; Krauss et al. 2014). An investigation into the global mangrove extent over the past 10,000 years suggests that mangroves cannot survive when SLR exceeds 6.1 mm/year (Saintilan et al. 2020). As current projections estimate that SLR rates could exceed 10 mm/year by 2100 (Church et al. 2013; Fox-Kemper et al. 2021; Kopp et al. 2014), effective modeling approaches that can help identify thresholds for ecological transformation and migration options with SLR are essential.

Mangrove forests are essential ecosystems that serve as habitats for diverse species and offer valuable ecosystem services to humans. Some communities depend heavily on mangroves for sustenance, materials, and energy (Naylor et al. 2002). Mangrove forests are a primary food source and provide livelihoods for communities as a cultural tradition, including the harvest of shellfish, crabs, and fish (Mitra 2020). Mangroves not only offer significant ecological benefits but also provide crucial protective functions, particularly during tropical cyclones and tsunamis (Dahdouh-Guebas and Pulukkuttige 2009; Danielsen et al. 2005). On a global scale, mangroves play a crucial role in mitigating climate change by sequestering and storing more carbon from atmospheric carbon dioxide (CO_2) per unit area than any other tropical forest ecosystem (Donato et al. 2012). Understanding relative mangrove vulnerability to SLR across a range of spatial scales will help facilitate more effective management that may mitigate the SLR-induced reductions in ecosystem services.

The response of mangroves to SLR is influenced by a complex interplay among biological and physical factors, along with landscape modification from people. Important factors include tidal range, suspended sediment loading, freshwater input affecting root growth, ability to transgress inland or horizontally, and the initial condition of the mangrove forest, all of which contribute to their vulnerability or resilience to SLR (Lovelock et al. 2015; MacKenzie et al. 2016). Mangroves can maintain their relative elevation through various accretion processes, including root growth, sedimentation, and peat development (Krauss et al. 2014). Additionally, mangroves possess the capability to transgress upslope to counteract SLR and maintain their elevation relative to ocean levels (Krauss et al. 2011). Together, these vertical and horizontal processes contribute to the resilience of mangroves to SLR. It is also important to note that human-induced alterations to the landscape such as roads and bridges and deforestation can disrupt these processes critical for accretion and physically impede the upland transgression of mangrove forests. Mangroves are already affected by deforestation and development (Gattuso et al. 2015) and large-scale die-offs have been observed with landscape and hydrological modifications (Gauthey et al. 2022).

There have been many efforts to project tidal marsh biogeomorphic changes with SLR (e.g., Craft et al. 2009; Fagherazzi et al. 2012; Langston et al. 2020; Morris et al. 2002; Swanson et al. 2014). Numerical models of tidal marsh accretion processes and response to projected SLR suggest that resilience is largely dependent on local or regional factors, particularly sediment availability, tidal range, rates of organic matter accumulation, and the slope of adjacent uplands (Buffington et al. 2021; Carr et al. 2020; Coleman et al. 2021; Langston et al. 2020; Thorne et al. 2018). However, despite numerous similarities in the underlying processes that drive changes in tidal marshes and mangrove forests, mangroves have not been treated with the same attention. Instead, mangrove modeling has generally focused on individual-based concepts (e.g., Berger et al. 2008), the dynamics of forest growth (Berger and Hildenbrandt 2000; Chen et al. 1998; Jiang et al. 2012), physiological functions (e.g., Asaeda and Kalibbala 2009), or coastline evolution (e.g., van Maanen et al. 2015). A revised version of MEM (CWEM) does allow simulations of both marsh and mangroves, although without a competition component (Morris et al. 2023).

Climate adaptation and planning is important given the uncertainty of future greenhouse gas emissions in SLR and associated influences that SLR may have on altering complex ocean-ecological processes. An Intergovernmental Panel on Climate Change report identified small islands as one of the main areas of concern, where understanding climate change impacts, adaptation potential and options, and overall vulnerability in the near-term is a high priority (Mycoo et al. 2022). Herein, we describe a new, flexible modeling framework for simulating mangrove responses to SLR and identify thresholds for vulnerability. Our approach draws inspiration from existing models used in tidal ecosystems, such as REM (Rybczyk et al. 1998), NUMAN (Chen and Twilley 1999), MEM (Morris et al. 2002), WARMER (Swanson et al. 2014), and WARMER-2 (Buffington et al. 2021). Our approach (WARMER-3) incorporates key factors that influence soil elevation, including species community composition, tidal flooding frequency, organic and mineral sediment composition, root growth, and tidal range. As the first case study for the model, we selected a location with robust datasets that is lacking in local projections of SLR vulnerability. Our specific objectives were to (1) explore SLR vulnerability across seven drainage basins on the Pacific Island of Pohnpei, Federated States of Micronesia,

(2) identify a SLR threshold for mangrove forest submergence, and (3) conduct a sensitivity analysis to determine what model parameters influenced the results the most. Our framework is unique in that it can simulate the interactions of multiple species, leveraging species-specific parameters when available, while tracking the fate of belowground organic matter that influences elevation change and carbon accumulation.

Methods

Model Development

We developed a general, 1-D modeling framework for simultaneous simulation of tidal wetland soil processes and species interactions with sea-level rise (Fig. 1). WARMER-3 uses a cohort approach to track soil organic and inorganic material through time, at an annual timestep, and space (soil depth). Twelve soil depth cohorts are used in this model; material transfers to deeper cohorts at differential rates such that the top 11 cohorts maintain a constant soil depth interval (5, 10, 10, 10, 10, 10, 10, 20, 20, 40, 100 cm), while the deepest cohort accumulates volume. The model is relatively insensitive to the size distribution of cohorts, allowing flexibility in the resolution of belowground processes. The processes that contribute to the organic soil pool include root turnover (three size classes), litterfall (branches and leaves), and decomposition; organic material was separated into labile and refractory pools subject to different rates of loss. Surface mineral deposition was simulated using a point model that considers tidal depth and dynamic suspended sediment concentrations in the water column (Buffington et al. 2021; Marani et al. 2010). The model is relatively detailed in tracking the fate of multiple organic matter pools; this was done to facilitate the independent calibration of the various processes that may influence elevation change. Both mineral and organic accumulation rates as well as overall accretion rate from dated soil cores are used for calibration.

The model framework is flexible to handle any number of species or functional groups. Carrying capacity and growth rates are defined in terms of basal area density (m^2/m^2). Species can expand their fraction of carrying capacity at a rate constrained by their maximum growth rate, environmental conditions (relative distribution across flooding regimes), and available space. Mortality is initiated by changes in flooding outside the preferred range. For simplicity, flooding duration is the only factor that defines the niche of each species; further development is ongoing to account for species responses to changes in salinity, but salinity constraints are

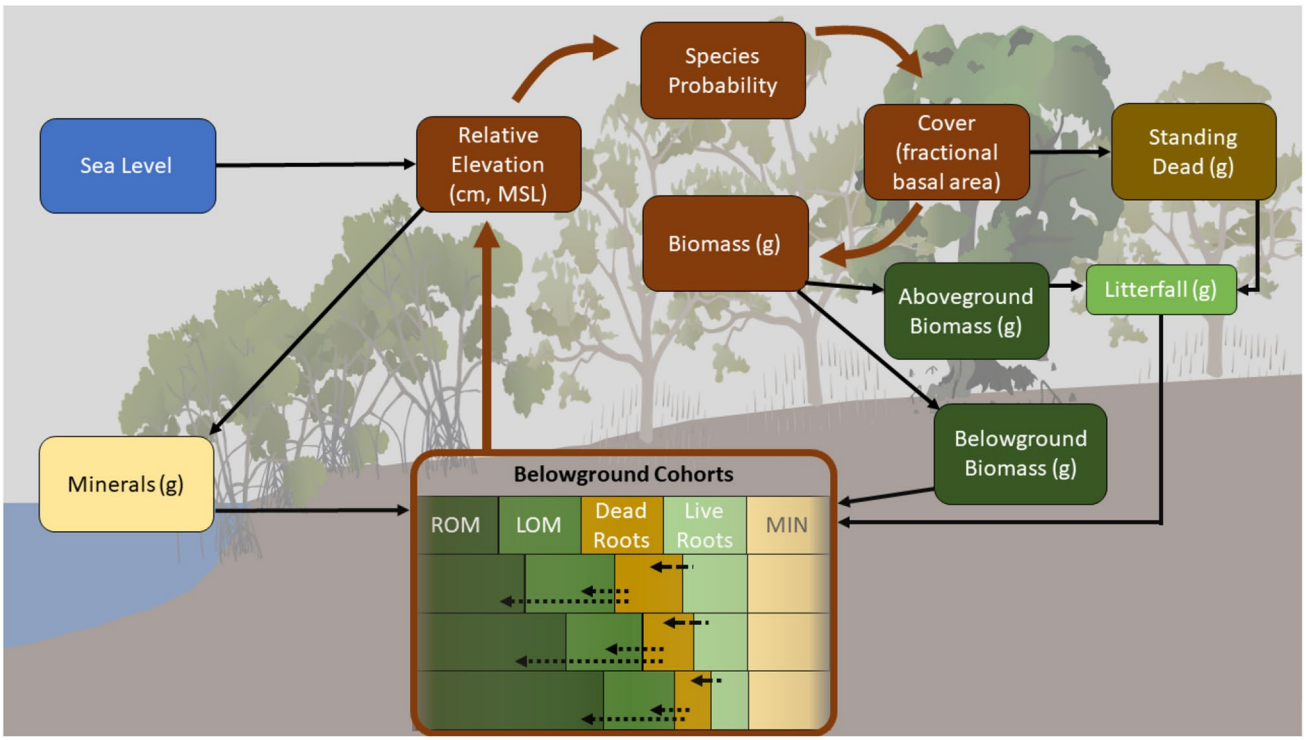

Fig. 1 Conceptual diagram for the approach to simulating surface-elevation dynamics relative to sea-level rise by modeling above and belowground organic and mineral pools and their associated processes in mangrove forests. MSL: mean sea level; ROM: refractory organic material; LOM: labile organic material; MIN: mineral sediments. Mangrove images from the IAN library (https://ian.umces.edu/media-library/)

limited in Micronesian high island mangroves (Ewel et al. 1998).

Allometric equations and empirical relationships were used to convert basal area density (m^2/m^2) to aboveground organic material (g/m^2). By linking basal area and biomass, we assumed that basal area increases with age (Phan et al. 2019). Aboveground biomass was subsequently transferred into the belowground soil cohorts via root-to-shoot ratios (Komiyama et al. 2008), with an exponential decay rate down to the maximum rooting depth. Root productivity was assumed to be in equilibrium with root turnover. The volume of the surface cohort was defined by an empirical relationship between bulk density and percent organic matter (Morris et al. 2016). In subsequent cohorts, volume was defined by a model of porosity, or void space, whereby porosity decreased as the density in overlaying cohorts increased; mineral and organic matter was assumed to have constant densities (2.65 and 1.14 g/cm^3, respectively). Rates of soil consolidation were controlled by a compaction rate term that defined how quickly porosity decreased downcore. Root collapse due to mortality was also simulated; dead roots have higher density than live roots, accounting for the collapse of aerenchyma tissue, with species-specific root porosity. While the model was developed specifically for mangroves, marsh species can also be included, for example, by relating aboveground biomass to stem diameter and density. See the Supplemental Information for equations and complete model description.

Study Site

The Federated States of Micronesia (FSM) consist of four main island states located approximately 4000 km (km) southwest of Hawaii, just north of the equator. Our study site Pohnpei is the largest island state in the FSM, spans 346 km^2, and is home to around 35,000 people. Its terrain is characterized by steep slopes rising from the coast to the summit of a dormant volcano, reaching nearly 800 m (m) in elevation. Pohnpei is surrounded by coral reefs and encompasses 57 km^2 of mangroves in its coastal lowlands, which serve as crucial habitat for endangered species such as the Pohnpei lorikeet (*Trichoglossus rubiginosus*) and fruit bat (*Pteropus molossinus*). Mangroves also play a substantial role in supporting the livelihoods of local communities throughout the FSM as they provide a source of income through fishing, crabbing, and fuelwood harvesting, contributing to the equivalent of more than half of the annual household income (Naylor et al. 2002). We conducted our analysis using data for the five most common mangrove species on Pohnpei: *Bruguiera gymnorrhiza* L., *Rhizophora apiculata* Blume, *Rhizophora stylosa* Griff. (inclusive of *R.* × *lamarckii* Montrouz), *Sonneratia alba* Sm., and *Xylocarpus granatum* J.Koenig (Fig. 2).

Pohnpei experiences a tropical rainforest climate, being one of the wettest places on Earth with an average annual rainfall of 480 cm and no distinct dry season (Lander and Khosrowpanah 2004). El Niño–Southern Oscillation (ENSO) is a major driver of interannual rainfall variability, resulting in drier conditions during the post-El Niño years. ENSO also affects sea level due to ocean temperature and currents, with possible changes of ± 30 cm (cm) during an ENSO event (Ellison et al. 2022; Lander and Khosrowpanah 2004).

Calibration Datasets

The model leverages various field datasets for calibration and validation, including dated soil cores, forest inventory surveys, elevation change data from surface elevation tables (SETs), and water-level records from gauges deployed across Pohnpei. We selected seven representative sites across Pohnpei to assess resilience to SLR, leveraging accretion rate data derived from 29 1-m deep cores from across the seven sites that were dated using lead–210 (MacKenzie et al. 2024; Fig. 3). Accretion rates, mineral accumulation rates, and organic accumulation rates for each site were used for calibration (Table 1).

We used site-specific water level records (Ellison et al. 2022) and a long-term gauge located near the Pohnpei International Airport (code, PNI) to calculate mean sea level (MSL), mean high water, and mean low water for 1983–2001, the most recent National Oceanic and Atmospheric Administration (NOAA) epoch. For sites without water-level data (Pwudoi, Palikir, West Sokehs), the MSL was assigned according to the nearest site with data (Table 1).

To ensure consistency across all field datasets, we conducted elevation surveys at each study site to establish a common vertical datum. Temporary benchmarks were set up outside the mangrove forest using a Trimble global navigation satellite system base station. Differential leveling was then used to determine the elevation from the benchmark to the SET and soil-core locations at each site. Additionally, we recorded the presence of each mangrove species within a 10-m radius at each turning point along the leveling transect. Species-elevation data from 152 plots were used to derive probability distribution functions for each species, which subsequently influenced the growth rate in the population model (Fig. 4). Further, the soil core elevations were used to calibrate a site-specific mineral deposition function.

We used a multi-step calibration approach to estimate crucial parameters while accounting for site-specific differences (Table S1). Four parameters were allowed to vary for site-specific model calibration. First, the mineral accumulation rate was calibrated based on data from soil cores. Second, the carrying capacity, defined as basal area density, was

Fig. 2 Dominant mangrove tree species of Pohnpei, Federated States of Micronesia. The structure of the trunks and pneumatophores vary between species along with their salinity and flooding tolerance (photo credits: Ken Krauss (*S. alba*) and Kevin Buffington (others), U.S. Geological Survey)

calculated as the 95th percentile from forest inventory plot surveys conducted in each region. The maximum soil porosity was held at a constant 0.88 across sites, but the minimum soil porosity was determined through calibration with the available soil core data. Lastly, the rates of decomposition were calibrated to minimize the discrepancy between modeled and observed accretion across 50 years of simulation, using the historic sea-level rise rate (3.75 mm/year, Ellison et al. 2022) and initial elevations estimated from soil core accretion rates. Model-predicted values of live and dead root biomass, living roots (fine and coarse), and the ratio of dead to live roots were compared with values from Cormier et al. (2015) and generally fell within the range of literature values for all sites after parameter tuning (see Appendix 1, Supplemental Information).

The framework can handle species-specific differences in all biotic parameters; however, due to a lack of species-specific information, only growth rates (Table S2), wood density and standing biomass (Tables S3 and S4), and the elevation niche (Fig. 4) were varied in the model across species. The proportion of structural roots was calibrated such that the mass pools of living fine and large roots were within the range of values from FSM (Cormier et al. 2015), assuming that structural roots and pneumatophores were not included in the soil cores of that study. The model does not explicitly consider the effects of salinity or macronutrients on organic deposition or decomposition and instead assumes that site-specific values of carrying capacity and organic accumulation rate from soil cores reflect these factors (Table S5). The lower elevation limit for mangrove survival was set at −0.57 m relative to MSL, a value determined from surveys around the island (Ellison et al. 2022), while the lower limit for mangrove seeding was set to 75% flooding duration (Krauss et al. 2006). To calibrate the model, a 200-year spin-up period was employed to develop the soil core and mangrove species composition for each initial elevation, followed by a 50 year hindcast using relative sea-level rise rates equal to the historic rate of 3.75 mm/year. The initial elevation of each soil core was calculated from the accretion rate and the sea-level rise amount over 50 years to account for the change in relative elevation. We then compared modeled and observed mineral and organic matter accumulation rates, overall vertical accretion, and final elevation.

Implementation

We used a 200-year model spin-up to develop the forest and soil profile, holding each initial elevation (−55 to 110 cm MSL in 5 cm increments) constant. Relative species basal area across each site was used to parameterize the

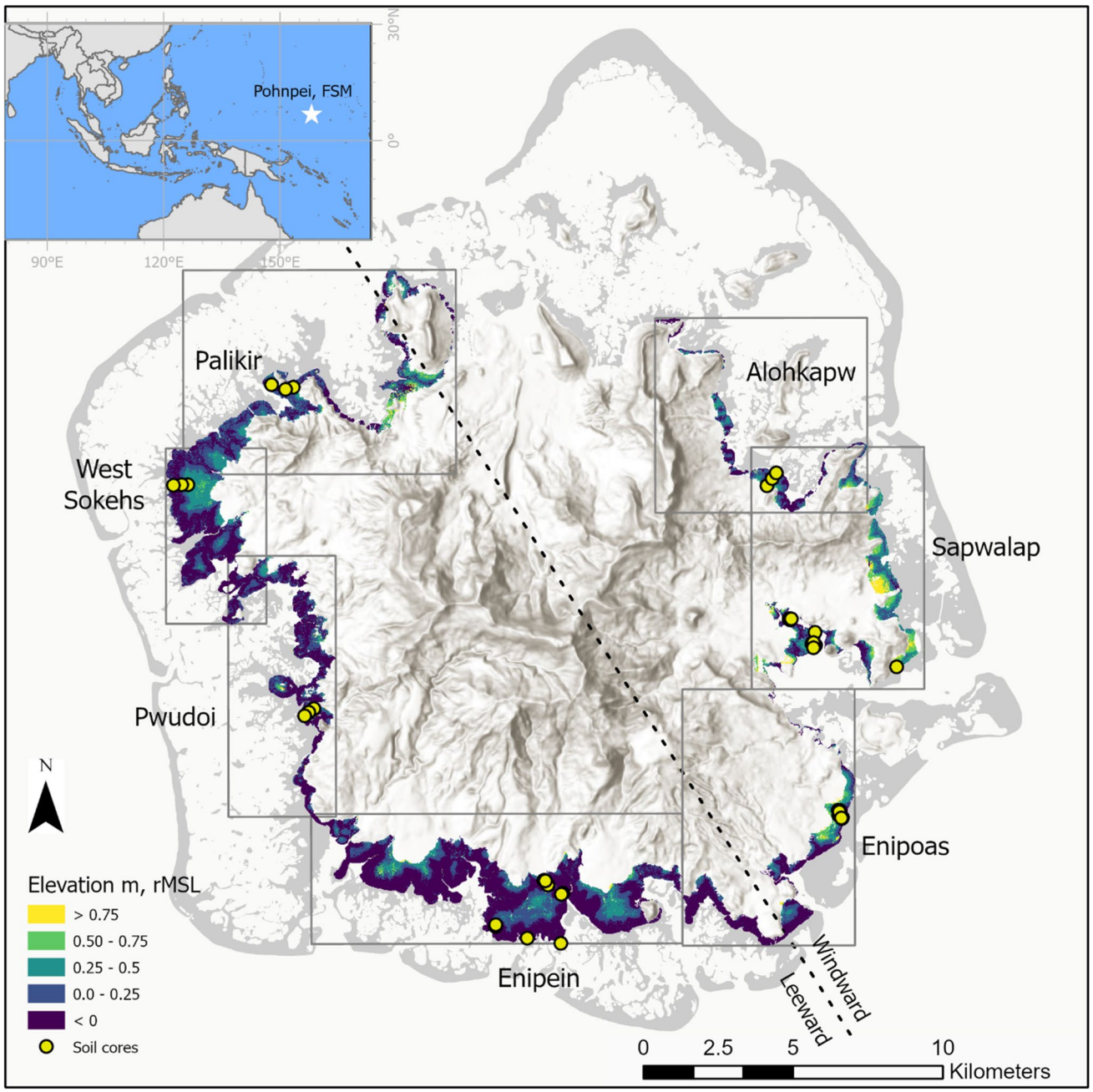

Fig. 3 Location and digital elevation model, relative to local mean sea level (rMSL), of study sites around Pohnpei, Federated States of Micronesia. Yellow points represent locations of soil core data used to calibrate the model. Created in ESRI ArcGIS Pro 3.3.0; basemap from ESRI

competition term so that species composition over the spin-up period reflected site conditions; after spin-up, competition was informed by the island-wide relative basal area for each species. The sea-level rise scenarios were then simulated after the spin-up period. Uncertainty in model projections was assessed using 1000 iterations of a Monte Carlo (MC) framework, with important model inputs (water level, suspended sediment concentration (SSC), and the decomposition rate; Table S6) sampled randomly. Distributions of mineral deposition and the decomposition rate (mean ± S.D.) were determined for each site by calibrating to each soil core. For each MC simulation, both SSC and the decomposition rate were sampled from a normal distribution. We interpolated the 1-D model projections from each MC run across a digital elevation model (DEM) derived from an airborne lidar survey flown in July 2023 that utilized a full waveform sensor (D. Comer, pers. comm). Site-specific MSL was then subtracted from the orthometric height DEM, creating

Table 1 Mean (SD) soil core accretion rates, organic and mineral accumulation rates, and soil core elevation, along with the regional mean sea-level estimate for study sites on Pohnpei, Federated States of Micronesia. From MacKenzie et al. 2024

Site	n	Accretion (cm/yr)	Organic accumulation ($g/m^2/yr$)	Mineral accumulation ($g/m^2/yr$)	Soil core elevation (m, EGM2008 geoid)	Mean sea level (m, EGM2008)
Alohkapw	3	0.361 (0.130)	402.9 (110.8)	1054.9 (759.6)	1.249 (0.0298)	1.023
Enipein	2	0.265 (0.147)	330.6.6 (151.3)	299.1 (109.3)	0.843 (0.066)	0.816
Enipoas	7	0.272 (0.092)	337.5 (105.0)	145.6 (45.1)	1.038 (0.029)	0.905
Palikir	3	0.424 (0.019)	454.8 (70.1)	220.8 (36.9)	0.935 (0.006)	0.905
Pwudoi	3	0.207 (0.107)	324.3 (159.3)	114.9 (56.0)	0.859 (0.078)	0.816
Sapwalap	9	0.369 (0.331)	472.7 (507.5)	521.2 (470.3)	1.175 (0.071)	0.905
West Sokehs	2	0.157 (0.036)	250.8.5 (127.6)	66.4 (7.4)	1.075 (0.017)[a]	0.905

[a]Elevation estimated from digital elevation model at West Sokehs

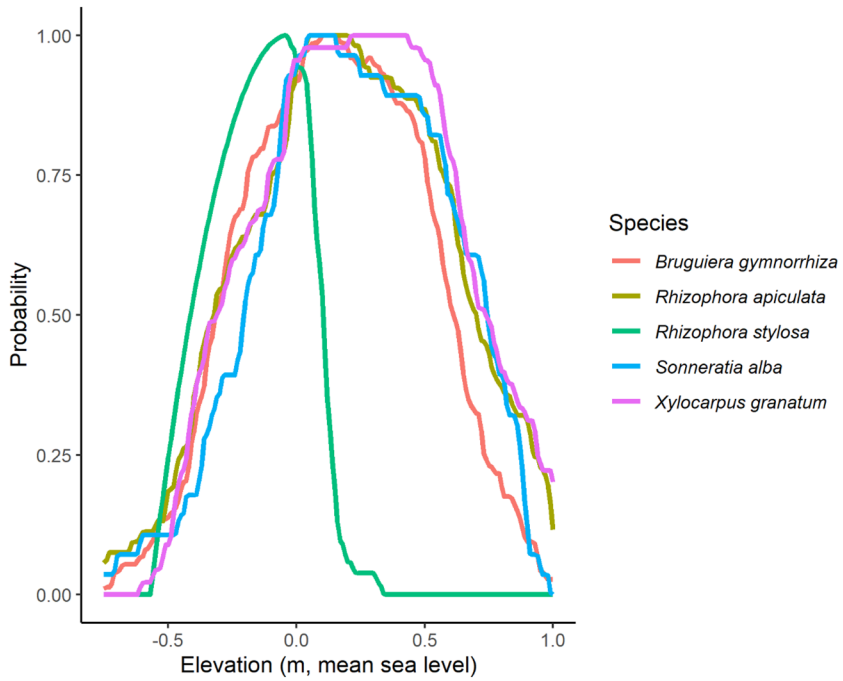

Fig. 4 Elevation (in meters relative to mean sea level) probability distribution functions for five common mangrove species on Pohnpei, Federated States of Micronesia. Curves were informed by field surveys of species distributions

a surface relative to local tidal flooding. The DEM was then clipped to the current extent of mangrove forest (Woltz et al. 2022), which provided the initial elevation distribution.

Wetlands that develop in areas with larger tidal ranges are known to exhibit higher resilience to sea-level rise due to their ability to build soil-surface elevations (Coleman et al. 2021; Kirwan et al. 2010). These wetlands also tend to have more time before being submerged by sea-level rise, especially if they are located further inland (Lovelock et al. 2015). To account for the effects of ENSO on water level MSL in our future projections, we applied a statistical approach. We first fitted a second-order polynomial to the 45-year record of MSL from Pohnpei to remove the local trend in sea-level rise. Next, we fitted a Weibull distribution to the residuals from the regression, representing the recent historic influence of ENSO, storms, and long-period lunar nodal harmonics. We then sampled from the Weibull distribution each year and added the residuals to the sea-level rise scenario. To summarize the projected results, we calculated the mean annual elevation relative to MSL, distributions of species cover, and rates of carbon accumulation. Final model runs were conducted with the USGS Hovenweep supercomputer (Falgout et al. 2024).

Validation

We used a SET (surface elevation table) record from 1999 to 2019 to independently validate the model (SET locations described in Krauss et al. 2010). At Sapwalap and Enipoas, we used data from three replicate SETs in fringe, riverine, and interior hydrologic zones. Using the differential survey elevation data, we calculated the absolute elevation of each

pin measurement relative to the Earth Gravitational Model of 2008 (EGM2008) datum and determined the elevation in 1999. We employed the same 200-year model spin-up scheme to establish the mean initial soil profile and mangrove community at the elevation of each SET. The observed annual change in mean sea level at the Pohnpei Harbor gauge was used to force the model. We then compared the average modeled and observed accretion rates for the 20-year period from 1999 to 2019.

Sea-Level Rise Scenarios

To evaluate the future vulnerability of mangrove forests in the vicinity of Pohnpei up to 2150, we used six different sea-level rise scenarios from the IPCC 6th assessment report. Local projections for Pohnpei were obtained from the NASA Sea Level Rise Projection tool, with the median projection selected for each scenario (Garner et al. 2021). To assess how SLR rate thresholds varied by site, we ran linear SLR scenarios (2–14 mm/year at 0.25 mm/year intervals) for each site using the mean elevation, average of parameters, and no variation in MSL. These runs involved a 200-year model spin-up to establish the initial soil cohort and forest, followed by a 200-year simulation. Mangrove cover (> 50%) at the end of the simulation was used to determine the SLR threshold for each site.

Sensitivity

Sensitivity to 24 model parameters was determined through a metamodeling exercise. Parameter values were randomly selected from a range (± 20% of mean parameter values) and used in an 81-year simulation (2020–2100) across three sea-level rise scenarios (40, 80, and 120 cm by 2100). For each set of randomly generated parameters, the model was run across a range of initial elevations (10, 20, 30 cm relative to MSL); this process was repeated 50,000 times. For each SLR scenario, the resulting mean accretion rates in the last 25 years of the simulation were used as response variables in a random forest (RF) model, with the input parameter values as predictors. The RF model was validated against 10% of the data that was withheld from training; RMSE for predicting accretion was 0.41 mm/year ($R^2 = 0.81$). We then calculated relative predictor importance as an indicator of model sensitivity (Table S7).

Results

Model validation using independent SET measurements at Sapwalap and Enipoas demonstrated good agreement with model projections, despite the model not accounting for spatial dynamics, such as distance from sediment source. Across Sapwalap fringe, interior, and riverine SETs, the average accretion rate was 2.28 ± 2.27 mm/year (range: 0.06–4.66 mm/year, 1999–2019). The model projected a similar average accretion rate of 2.35 ± 0.34 mm/year over the 20-year simulation period from 1999 to 2019, based on the initial elevation from each SET. At Enipoas, the average SET accretion rate was 1.56 ± 0.69 mm/year (range: 0.55–2.71 mm/year), and the model projected an average accretion rate of 3.05 ± 0.48 mm/year. The average model rates were close the observed ranges at both sites, overpredicting accretion by 0.08 mm/year at Sapwalap and by 1.49 mm/year at Enipoas.

During the 131-year period from 2020 to 2150, the model projected a decline in average elevation relative to MSL at all sites (Fig. S2). Substantial changes in community composition were projected after 2050 under higher sea-level rise scenarios or after 2075 for lower sea-level rise scenarios (Figs. 5, S3, and S4). By 2150, total extent of mangroves was projected to be reduced by nearly half (41.3 ± 4.8%) in the SSP 1–1.9 SLR scenario, a 60.6 ± 4.3% reduction under the SSP 1–2.6 scenario, and 71.9 ± 6.3% reduction under the SSP 2–4.5 scenario (Fig. 6). For the SSP 3–7.0 scenario, mangrove area begins to decline around 2080, with an 88.7 ± 3.4% reduction in area by 2150. Under SPP 5–8.5, mangrove area starts to decline by 2075, with a 93.4 ± 2.1% reduction in area by 2150. The highest SLR scenario, SSP 5–8.5 low confidence, rapid declines in mangrove area were projected to start in 2072, with a 99.9 ± 0.32% reduction in mangrove area by 2150.

There were differences in projected response to SLR across the seven study sites (Fig. S3). Areas on the leeward side of the island tended to be more vulnerable to sea-level rise than areas on the windward side (Figs. S3-S4), due primarily to higher sediment availability and elevation capital at Alohkapw and Sapwalap. The susceptibility to sea-level rise at West Sokehs, Pwudoi, and Enipein was primarily attributed to low rates of mineral and organic accumulation and relatively low elevation capital (Table 1).

The changes of community composition showed similar patterns across sites, with higher rates of SLR leading to faster decreases in the cover of species intolerant of extended flooding (Figs. S3-S4). *Bruguiera gymnorrhiza or S. alba* were projected to have high initial cover at all sites, which is consistent with field-survey data that show these species are broadly distributed, but with *S. alba* being more prevalent at windward sites; cover of these species declined across all sites and SLR scenarios. *Xylocarpus granatum*, which tends to grow in the upper end of the tidal zone, was projected to have low cover at all sites except Enipein, where it rapidly declined in cover across in all scenarios. *Rhizophora apiculata* had moderate to high cover initially at most sites but was projected to decrease in cover across all scenarios. *Rhizophora stylosa* is typically found in the coastal edges of the forest and relatively low in the tidal frame; WARMER-3

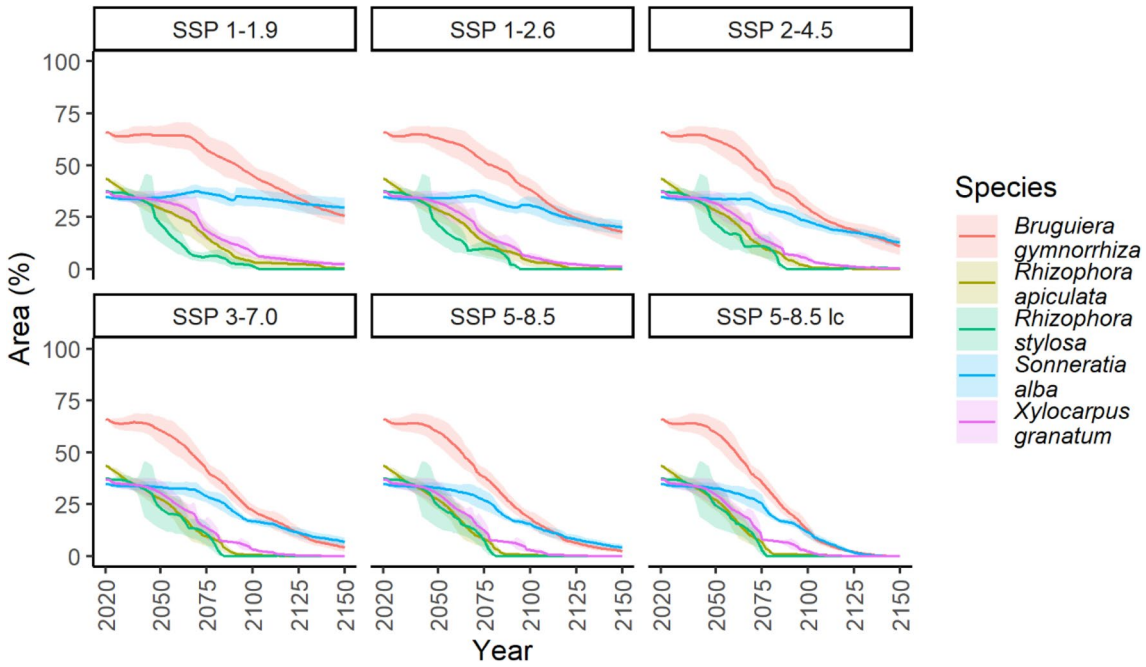

Fig. 5 Mean (±SD) mangrove tree species percent area coverage under six sea-level rise scenarios through 2150. Sea-level rise scenarios are organized from lowest (SSP 1–1.9) to highest (SSP 5–8.5 lc)

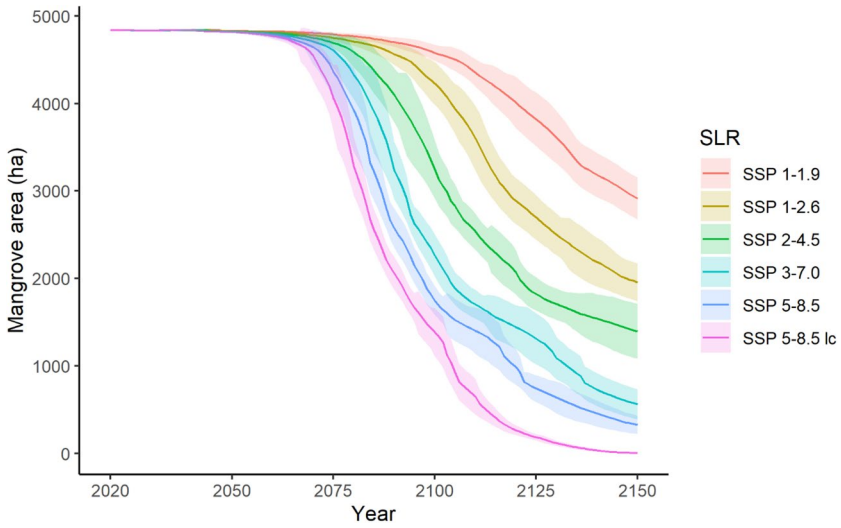

Fig. 6 Total mangrove area projected under six sea-level rise scenarios. Mangrove cover is stable through 2070 but begins to have a rapid decline after 2100 with sea-level rise acceleration. Shaded areas represent standard deviation generated by Monte Carlo simulations. Sea-level rise scenarios are organized from lowest (SSP 1–1.9) to highest (SSP 5–8.5 lc)

projected low cover across all sites except Enipein and West Sokehs, but cover was projected to decline across scenarios.

Projected rates of soil carbon accumulation were highly variable, but on average they declined for all SR scenarios from a peak of 1.49 ± 0.77 Mg C ha^{-1} yr^{-1} at the start of simulation. Under the lower two SLR scenarios, net carbon accumulation remained positive through 2150 (0.42 ± 0.88, 0.21 ± 0.81 Mg C ha^{-1} yr^{-1} for the respective scenarios) as accommodation space widens. However, under the higher four scenarios, loss of mangrove cover resulted in a net release of carbon toward the end of the century (Fig. 7). The model was very sensitive to inputs that control the fate of organic matter.

We found that sites varied in their SLR threshold rate, beyond which the mangrove forest will likely submerge (Table S6). Pwudoi had the lowest SLR threshold at 6.0 mm/year, while Sapwalap had the highest at 11.75 mm/year. On average, the SLR threshold was 7.8 ± 2.2 mm/year across sites. The sensitivity analysis for the rate of elevation change indicated that carrying capacity and litter deposition rate

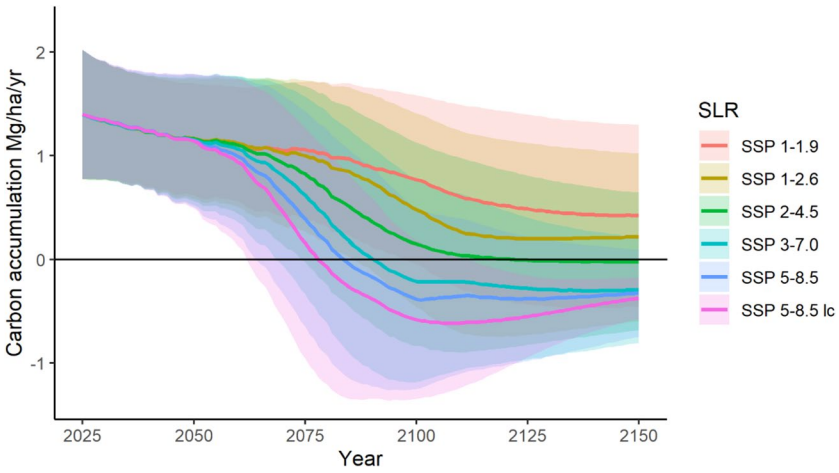

Fig. 7 Projected mean (±SD) rates of carbon accumulation for Pohnpei mangroves under six sea-level rise scenarios. Sea-level rise scenarios are organized from lowest (SSP 1–1.9) to highest (SSP 5–8.5 lc)

were the most important parameters, with a combined importance of 0.78. The decomposition rate and fraction of structural roots were the next most important parameters (Table S7). Together, these results highlight the importance of constraining parameters that control net organic matter accumulation rates.

Discussion

Mangrove Vulnerability

We conducted a scenario modeling approach to investigate tropical mangrove forest responses to SLR. The simulations suggest that there will be limited changes in forest community composition during the first 30 years across all SLR scenarios (Fig. 5), aligning with a recent study that found little coastline change in Pohnpei over the past two decades, despite relatively high SLR rates (Nunn et al. 2017). Our modeling projections indicate that mangroves surrounding Pohnpei are expected to exhibit some resilience in response to low (SSP 1–1.9) to moderate (SSP 2–4.5) SLR rates (Fig. 5). Under higher SLR rates (SSP 3–7.0 and above), however, WARMER-3 suggests a transition to flood tolerant tree species and eventually substantial loss of mangrove forest.

Our results demonstrated that regions of Pohnpei had variable resilience to SLR. Sapwalap, Alohkapw, and Palikir were the most resilient areas to SLR and maintained their elevations and forest composition the longest (Fig. S6). These sites had relatively high initial elevations within the tidal frame, or "elevation capital," which increased their resilience to SLR (Cahoon et al. 2019; Rogers 2021). Also, Alohkapw and Sapwalap are near large riverine drainages and had higher mineral sediment accumulation rates than other sites (Table 1), which also contributed to their vertical accretion and overall resilience. Variation in measured elevation changes was observed across different hydrodynamic settings in Pohnpei and Kosrae, FSM, with large riverine areas having the highest rates of elevation gain (Krauss et al. 2010).

Fluvial sediment may be responsible for increasing mangrove resilience to SLR across Pohnpei. Watershed area, steep topography, heavy rainfall, and human disturbance can combine to influence sedimentation rates. Forest clearing and other human activities upriver in island watersheds may be responsible for the elevated rates of sediment deposition, with seaward mangrove transgression observed over the last 40 years (Woltz et al. 2022). Even small-scale forest clearing for construction or crops (Raynor and Fownes 1991) may contribute to local sediment loads. Future studies of mangroves should account for differences in watershed characteristics, weather, and adjacent landscape modifications that can influence accretion processes and overall resilience. For example, in this region of the world, there is great uncertainty about whether climate change will result in a dryer or wetter future as it depends on overall tropical warming (1–3 °C; Widlansky et al. 2013), which could mean lower or higher riverine flows to deliver sediment to mangrove forests downstream.

Our domain did not include adjacent inland areas that may transition to mangroves by transgression; however, potential migration area is greatly limited due to the mountainous terrain of the island. Like many islands, Pohnpei has steep slopes that are characteristic of its volcanic history. Transgression of mangroves into adjacent upland ecosystem types has not been widely observed globally (compared to salt marshes, e.g., Kirwan and Gedan 2019; Raabe et al. 2012; Williams et al. 1999), but saltwater intrusion, storms, and land conversion commonly facilitate transgression of tidal wetlands into new areas (López-Medellín et al. 2011; Osland et al. 2018). Fringing wetlands at appropriate elevations for mangrove colonization have mostly already been colonized by mangroves or, for smaller areas, are being

managed for low-land agriculture therefore little opportunity for transgression remains. There may be opportunities on Pohnpei for upslope transgression via riverine corridors such as Alohkapw or Sapwalap.

Overall, our projections show that some mangroves are likely to be lost, either later this century or into the first half of the next, depending on which SLR scenario is realized. Loss of mangroves will likely have substantial impacts across Pohnpei, including a reduction in habitat for endemic species and increasing human exposure to the effects of storms and tsunamis. Considering the large portion of the human population that engages in subsidence fishing, the effects on the fishery may be the most profound consequence of mangrove loss for Pohnpei.

Sea-Level Rise Thresholds

Our modeling indicates that mangroves may persist well beyond 2150 on Pohnpei, albeit with altered tree species distribution, if rates of SLR are kept below 7.8 mm/year. For SLR rates over 7.8 mm/year, mangroves were unable to maintain elevation relative to MSL and eventually transition to an unvegetated open water state. Our mean SLR threshold was higher than the global average threshold value of 6.1 mm/year reported by Saintilan et al. (2020), but close to their average rate of 7.1 mm/year for far-afield sites that include the Federated States of Micronesia. Our projected timeline of submergence generally aligns with other mangrove SLR projections or vulnerability assessments (Lovelock et al. 2015; Spencer et al. 2016). For example, Lovelock et al. (2015) found that Indo-Pacific mangroves in areas with sediment availability > 2.5 mg/L are unlikely to be submerged by 2100. Our modeling showed that Pohnpei forests are relatively resilient and likely to persist beyond 2100, although with altered species composition. However, by 2150, all SLR scenarios showed that over half of the current mangrove area may be lost.

Sensitivity Analysis

The most sensitive model parameters for controlling rates of elevation change had direct or indirect control on net organic matter accumulation rates. Carrying capacity is directly related to the above- and belowground biomass standing stock, influencing the production of roots, while the litter deposition rate is tied to carrying capacity and influences the soil composition of the surface. WARMER-3 was also relatively sensitive to the decomposition rate of labile and refractory organic particles; as this was one of the parameters randomly varied in the Monte Carlo projections, it is likely responsible for much of the variation in projected elevation. The large amount of variation in the projections of carbon accumulation also highlights the need for leveraging site and species-specific information. Constraining the compaction rate and minimum porosity with data, via direct calibration with accretion rates or informed by depth profiles of bulk density, is critical when implementing the model. In our analysis, the most vulnerable regions to SLR were West Sokehs, Enipein, and Pwudoi, which are all located on the leeward side of the island. Compared with the other regions, these areas had relatively low initial elevation and limited sediment availability, which translated to greater vulnerability under the SLR scenarios. Considering the projected high vulnerability to SLR and low measured accretion rates at some sites, additional investigation is warranted to better understand the spatial distribution of mangrove elevation relative to water levels, accretion rates, and sediment availability, which would help inform future SLR vulnerability assessments.

Resilience to SLR was bolstered by high productivity and rapid rates of organic soil accumulation, perhaps related to the large amount of rainfall Pohnpei experiences that moderates pore water salinity (16.1 ppt; Cormier et al. 2015). Changes in environmental conditions such as drought or changes to the sediment regimes could alter the rates of organic or mineral accumulation, resulting in reduced vertical accretion and greater vulnerability to rising seas. Such changes have been observed globally where extensive fragmentation of mangrove forests has occurred for agriculture and other landscape modifications (Bryan-Brown et al. 2020) and along Pacific rim nations coping with reduced sediment input to mangroves (Lovelock et al. 2015). In China, and elsewhere, aggressive mangrove conservation and restoration have been used to restore degraded ecosystems (Jia et al. 2018), and community-based approaches for restoration have been successful in Colombia (Rodríguez-Rodríguez et al. 2021). However, preserving the current condition of much of FSM's mangroves is far more cost-effective than promoting change that will necessitate future rehabilitation efforts (Lewis et al. 2016) and may be a good option for FSM given the cultural connection to the land.

Modeling Considerations

We made several simplifying assumptions and omitted some processes during our application of the model to Pohnpei's mangroves. While much data were available from historic US, Japanese, and local governmental efforts, we still had to use some off-island data to initialize our model. We focused on the above and belowground processes that control elevation and mangrove response to changes in flooding from SLR. Water and soil salinity can be a dominant driver of tidal wetland community composition and productivity (Ahmed et al. 2022; Sherman et al. 2003); however, due to lack of field data and specific knowledge of species responses, this was not incorporated in our approach. We know more about the seedlings

of these species (e.g., Allen et al. 2001; Krauss and Allen 2003) than we do mature trees here and in most mangrove forests where glasshouse studies have dominated individual species stress-response studies (Krauss et al. 2007). Similarly, the macronutrients nitrogen and phosphorus are known to play an important role in limiting mangrove growth in the Caribbean (Castañeda-Moya et al. 2013); nutrients were not included in Pohnpei simulations to reduce model complexity and lack of calibration data. However, to some degree, the effects of both salinity and nutrients are captured in the elevation distributions for each species and, at a regional scale, by basal area distributions derived from forest inventory plots. Nutrients have also not previously been judged to be especially limiting to Pohnpei's mangroves (Cormier et al. 2015) or on other islands in FSM (Ewel et al. 1998). By calibrating the model with soil-core accumulation rates from Pohnpei, we are assuming that the relationships among basal area, rates of productivity, and decomposition over the last century are representative of future conditions. Human development and climate change could both cause changes in the environment that affect mangrove productivity. For example, changes in freshwater delivery or sediment loading could have a strong effect on the health and persistence of mangroves as mangroves preferentially take up freshwater whenever possible (Ewe et al. 2007; Lovelock et al. 2017). Increased atmospheric carbon dioxide concentrations may also boost productivity of mangroves, potentially increasing their resilience to SLR through elevated root growth (Reef et al. 2016). We contend that on Pohnpei, while global environmental change continues to affect Pacific high islands from mountain tops to reefs, local impacts are relatively isolated and of the subsistence nature (Allen et al. 2001).

Elevation relative to tidal flooding is a key predictor of species presence. Species distributions relative to elevation have been documented for many mangrove species (e.g., Ellison et al. 2022; Leong et al. 2018); we developed these specifically for common Pohnpei species. However, one of the greatest sources of uncertainty for projections of future mangrove extent is the lack of accurate elevation data. Lidar is not available for many small Pacific islands, and due to incomplete penetration of the canopy, lidar-derived bare earth DEMs can have large vertical bias that require ground surveys and correction models to address (Buffington et al. 2016; Hladik and Alber 2012). We had access to both a robust lidar dataset and data from field surveys to validate DEM accuracy. Developing accurate elevation models is critical as elevation capital is particularly important when projecting future resilience. Pohnpei, like many small islands, did not have an accurate nearshore bathymetry dataset; thus, our modeling domain included only the current mangrove extent without nearshore attributes. It is possible that mangroves could prograde into adjacent reef habitats in some areas with excess sediment or sheltered from waves, as they have along specific rivers on Pohnpei in the past (Woltz et al. 2022), but this process was not considered in our application.

By design, WARMER-3 relies heavily on field measurements to generate site-specific projections. While this approach limits model application to areas with relatively robust datasets, we believe a solid understanding of local conditions—which we have for Pohnpei and/or adjacent islands—is necessary for projecting system behavior into the future with any confidence. Similar assessments for salt marshes have been successful in identifying estuaries that are relatively vulnerable to SLR (e.g., Thorne et al. 2018). Additional efforts to account for other aspects of climate change including increasing CO_2, temperature, and precipitation variation in models of wetland resilience are also needed.

Management Implications

Models can help policy and conservation groups seek attention and funding to implement adaptation strategies, especially when driven by local datasets. It has taken several decades of iterative wetland research to understand how SLR might impact Pohnpei's mangroves. Locally calibrated models that result from these studies can be used by resource managers to understand vulnerability and reduce uncertainties in future mangrove forest change under SLR scenarios. Continued monitoring and reassessment of the forest health over time on Pohnpei would further inform planning.

A critical consideration is how best to build resilience into mangrove ecosystems to prevent loss of mangroves and the services they provide. For small islands, rising sea levels could negatively impact their subsistence lifestyle and economy (Naylor et al. 2002), across FSM and throughout the Pacific. Food and water security will likely be more difficult to maintain if mangrove losses, or species' shifts, are realized over the coming decades. For example, as even lower SLR scenarios project that *X. granatum* will become less common on Pohnpei, a handicraft industry that peddles to tourists may be directly impacted. *Xylocarpus granatum* is preferred by wood carvers on Pohnpei, and the species' projected future demise with SLR aligns with its lack of regeneration in lower intertidal positions already brought on by greater salinity and flooding (Allen et al. 2003). Ecosystem-based SLR adaptation for mangroves may include facilitating upslope migration, improving connectivity, and implementing dedicated restoration projects (Sierra-Correa and Cantera Kintz 2015). Preferred mangrove species propagation may even become the target of small plantations, as is legacy in parts of Malaysia, for example (Watson 1928). Other mangrove species, such as *R. apiculata*, are also of particular value as a preferred cooking wood in Micronesia (Allen et al. 2001). Like *X. granatum*, the distribution of *R. apiculata* may decline with moderate accelerations in SLR.

Projecting the fate of mangrove forests is key to informing decision-making for natural resource managers and people concerned about the cultural and economic value to local communities. Through extensive calibration with empirical datasets, we developed future projections of mangrove community composition and elevation in response to SLR for the island of Pohnpei. Mangroves were projected to be resilient to low and moderate SLR scenarios, but extensive loss of suitable mangrove habitat could result if the high or extreme SLR scenarios are realized. The SLR rate threshold averaged 7.8 mm/year, in line with a recent global analysis. By developing a flexible model framework, and through calibration with extensive field datasets, we were able to develop local projections of mangrove resilience to SLR. The variation in vulnerability across sites demonstrates the utility of and need for local and species-specific data to make robust projections of an uncertain future.

Supplementary Information The online version contains supplementary material available at https://doi.org/10.1007/s12237-024-01422-y.

Acknowledgements The project was conceptualized by Chris Swensen at the U.S. Fish and Wildlife Service and Zhiliang Zhu at the USGS. For help with field work, logistics, or general information, we would like to thank Tamara Greenstone Alefaio (Micronesia Conservation Trust), Francisca Sohl, Angel Jonathan, Bejay Obispo, Kirino Olpet (Conservation Society of Pohnpei), Eugene Eperiam, Emos Eperiam, Bersin Elias, and Yosda Sailas (Pohnpei Department of Forestry). Additional contextual was provided by Joanna Ellison (University of Tasmania). We also would like to thank Elitsa Peneva-Reed (USGS Eastern Geographic Science Center) for her invaluable forest inventory dataset and to Dean Gesch, Jeff Irwin, and Jeff Danielson for their efforts collecting elevation data in the mangroves. Thanks also to Doug Comer and Jake Comer with Cultural Site Research and Management for providing access to the lidar dataset. Any use of trade, firm, or product names is for descriptive purposes only and does not imply endorsement by the US Government.

Funding This work was funded by Department of Interior (DOI) Office of Insular Affairs, U.S. Geological Survey (USGS) Ecosystems program, USGS Climate R&D program, and the DOI USGS Pacific Island Climate Adaptation Science Center (PICASC). Support was also provided by USGS Western Ecological Research Center.

Data Availability The code developed to assess mangrove responses to sea-level rise is available at https://github.com/kbuff/warmer3. The model results are available at ScienceBase (https://doi.org/10.5066/P904WVF5).

References

Ahmed, S., S.K. Sarker, D.A. Friess, Md. Kamruzzaman, M. Jacobs, Md.A. Islam, M.D.A. Alam, M.J. Suvo, Md.N.H. Sani, T. Dey, C.S.S. Naabeh, and H. Pretzsch. 2022. Salinity reduces site quality and mangrove forest functions. From monitoring to understanding. *Science of the Total Environment* 853: 158662. https://doi.org/10.1016/j.scitotenv.2022.158662.

Allen, J.A., K.C. Ewel, and J. Jack. 2001. Patterns of natural and anthropogenic disturbance of the mangroves on the Pacific Island of Kosrae. *Wetlands Ecology and Management* 9 (3): 291–301. https://doi.org/10.1023/A:1011125310794.

Allen, J.A., K.W. Krauss, and R.D. Hauff. 2003. Factors limiting the intertidal distribution of the mangrove species Xylocarpus granatum. *Oecologia* 135 (1): 110–121. https://doi.org/10.1007/s00442-002-1167-2.

Andersen, T., J. Carstensen, E. Hernández-García, and C.M. Duarte. 2009. Ecological thresholds and regime shifts: Approaches to identification. *Trends in Ecology & Evolution* 24 (1): 49–57. https://doi.org/10.1016/j.tree.2008.07.014.

Asaeda, T., and M. Kalibbala. 2009. Modelling growth and primary production of the marine mangrove (Rhizophora apiculata BL): A dynamic approach. *Journal of Experimental Marine Biology and Ecology* 371 (2): 103–111. https://doi.org/10.1016/j.jembe.2009.01.009.

Berger, U., and H. Hildenbrandt. 2000. A new approach to spatially explicit modelling of forest dynamics: Spacing, ageing and neighbourhood competition of mangrove trees. *Ecological Modelling* 132 (3): 287–302. https://doi.org/10.1016/S0304-3800(00)00298-2.

Berger, U., V.H. Rivera-Monroy, T.W. Doyle, F. Dahdouh-Guebas, N.C. Duke, M.L. Fontalvo-Herazo, H. Hildenbrandt, N. Koedam, U. Mehlig, C. Piou, and R.R. Twilley. 2008. Advances and limitations of individual-based models to analyze and predict dynamics of mangrove forests: A review. *Aquatic Botany* 89 (2): 260–274. https://doi.org/10.1016/j.aquabot.2007.12.015.

Bryan-Brown, D.N., R.M. Connolly, D.R. Richards, F. Adame, D.A. Friess, and C.J. Brown. 2020. Global trends in mangrove forest fragmentation. *Scientific Reports* 10 (1): 7117. https://doi.org/10.1038/s41598-020-63880-1.

Buffington, K.J., B.D. Dugger, K.M. Thorne, and J.Y. Takekawa. 2016. Statistical correction of lidar-derived digital elevation models with multispectral airborne imagery in tidal marshes. *Remote Sensing of Environment*. https://doi.org/10.1016/j.rse.2016.09.020.

Buffington, K.J., C.N. Janousek, B.D. Dugger, J.C. Callaway, L.M. Schile-Beers, E.B. Sloane, and K.M. Thorne. 2021. Incorporation of uncertainty to improve projections of tidal wetland elevation and carbon accumulation with sea-level rise. *PLoS ONE* 16 (10): e0256707. https://doi.org/10.1371/journal.pone.0256707.

Cahoon, D.R., J.C. Lynch, C.T. Roman, J.P. Schmit, and D.E. Skidds. 2019. Evaluating the relationship among wetland vertical development, elevation capital, sea-level rise, and tidal marsh sustainability. *Estuaries and Coasts* 42 (1): 1–15. https://doi.org/10.1007/s12237-018-0448-x.

Carr, J., G. Guntenspergen, and M. Kirwan. 2020. Modeling marsh-forest boundary transgression in response to storms and sea-level rise. *Geophysical Research Letters* 47 (17): e2020GL088998. https://doi.org/10.1029/2020GL088998.

Castañeda-Moya, E., R.R. Twilley, and V.H. Rivera-Monroy. 2013. Allocation of biomass and net primary productivity of mangrove forests along environmental gradients in the Florida Coastal Everglades, USA. *Forest Ecology and Management* 307: 226–241. https://doi.org/10.1016/j.foreco.2013.07.011.

Chen, R., and R.R. Twilley. 1999. A simulation model of organic matter and nutrient accumulation in mangrove wetland soils. *Biogeochemistry* 44 (1): 93–118.

Chen, R., R.R. Twilley, and R. Twilley. 1998. A gap dynamic model of mangrove forest development along gradients of soil salinity and nutrient resources. *Journal of Ecology* 86 (1): 37–51. https://doi.org/10.1046/j.1365-2745.1998.00233.x.

Church, J.A., P.U. Clark, A. Cazenave, J.M. Gregory, S. Jevrejeva, A. Levermann, M.A. Merrifeld, G.A. Milne, R.S. Nerem, P.D. Nunn, A.J. Payne, W.T. Pfeffer, D. Stammer, and A.S. Unnikrishnan. 2013. Sea level change, Chapter 13. In *Climate change 2013—The physical science basis—Contribution of the working group I to the fifth assessment report of the Intergovernmental Panel on Climate*

Change, ed. T.F. Stocker, D. Qin, K.D. Plattner, M. Tignor, S.K. Allen, J. Boschung, A. Nauels, Y. Xia, V. Bex, and P.M. Midgley, 1137–1216. Cambridge University Press.

Coleman, D.J., M. Schuerch, S. Temmerman, G.R. Guntenspergen, C.G. Smith, and M.L. Kirwan. 2021. Reconciling models and measurements of marsh vulnerability to sea level rise. *Limnology and Oceanography Letters*. https://doi.org/10.1002/lol2.10230.

Cormier, N., R.R. Twilley, K.C. Ewel, and K.W. Krauss. 2015. Fine root productivity varies along nitrogen and phosphorus gradients in high-rainfall mangrove forests of Micronesia. *Hydrobiologia* 750 (1): 69–87. https://doi.org/10.1007/s10750-015-2178-4.

Craft, C., J. Clough, J. Ehman, S. Joye, R. Park, S. Pennings, H. Guo, and M. Machmuller. 2009. Forecasting the effects of accelerated sea-level rise on tidal marsh ecosystem services. *Frontiers in Ecology and the Environment* 7 (2): 73–78. https://doi.org/10.1890/070219.

Dahdouh-Guebas, F., and J.L. Pulukkuttige. 2009. A bibliometrical review on pre- and posttsunami assumptions and facts about mangroves and other coastal vegetation as protective buffers. *Ruhuna Journal of Science* 4 (4): 28–50.

Danielsen, F., M.K. Sørensen, M.F. Olwig, V. Selvam, F. Parish, N.D. Burgess, T. Hiraishi, V.M. Karunagaran, M.S. Rasmussen, L.B. Hansen, A. Quarto, and N. Suryadiputra. 2005. The Asian tsunami: A protective role for coastal vegetation. *Science* 310 (5748): 643. https://doi.org/10.1126/science.1118387.

Donato, D.C., J.B. Kauffman, R.A. Mackenzie, A. Ainsworth, and A.Z. Pfleeger. 2012. Whole-island carbon stocks in the tropical Pacific: Implications for mangrove conservation and upland restoration. *Journal of Environmental Management* 97 (1): 89–96. https://doi.org/10.1016/j.jenvman.2011.12.004.

Ellison, J.C., K.J. Buffington, K.M. Thorne, D. Gesch, J. Irwin, and J. Danielson. 2022. Elevations of mangrove forests of Pohnpei, Micronesia. *Estuarine, Coastal and Shelf Science* 268: 107780. https://doi.org/10.1016/j.ecss.2022.107780.

Ewe, S.M.L., L. da Sternberg, and S. L., & Childers, D. L. 2007. Seasonal plant water uptake patterns in the saline southeast Everglades ecotone. *Oecologia* 152 (4): 607–616. https://doi.org/10.1007/s00442-007-0699-x.

Ewel, K.C., J.A. Bourgeois, T.G. Cole, and S. Zheng. 1998. Variation in environmental characteristics and vegetation in high-rainfall mangrove forests, Kosrae. *Micronesia. Global Ecology and Biogeography Letters* 7 (1): 49–56.

Fagherazzi, S., M.L. Kirwan, S.M. Mudd, G.R. Guntenspergen, S. Temmerman, A.D. Alpaos, and va de Koppel, J., Rybczyk, J. M., Reyes, E., Craft, C., & Clough, J. 2012. Numerical models of salt marsh evolution: Ecological, geomorhpic, and climatic factors. *Reviews of Geophyics* 50 (RG1002): 1–28. https://doi.org/10.1029/2011RG000359.1.INTRODUCTION.

Falgout, J.T., J. Gordon, and M.J. Davis. 2024. USGS Advanced Research Computing [USGS Hovenweep Supercomputer]. https://doi.org/10.5066/P9XE7ROJ.

Fox-Kemper, B., H.T. Hewitt, C. Xiao, G. Aoalgeirsdottir, S.S. Drijfhout, T.L. Edwards, N.R. Gollledge, M. Hemer, R.E. Kopp, G. Krinner, A. Mix, D. Notz, S. Nowicki, I.S. Nurhati, L. Ruiz, J.B. Sallee, A.B.A. Slangen, and Y. Yu. 2021. Ocean, Cryosphere and Sea Level Change. In *Climate change 2021: The physical science basis. Contribution of Working Group I to the Sixth Assessment Report of the Intergovernmental Panel on Climate Change*, ed. V. Masson-Delmontte, P. Zhai, A. Pirani, S.L. Connors, C. Pean, S. Berger, N. Caud, Y. Chen, L. Goldfarb, M.I. Gomis, K. Leitzell, E. Lonny, J.B.R. Matthews, T.K. Maycock, T. Waterfield, O. Yelkci, R. Yu, and B. Zhou, 1211–1362. Cambridge University Press.

Garner, G.G., T. Hermans, R.E. Kopp, A.B.A. Slangen, T.L. Edwards, S. Levermann, S. Nowikci, M.D. Palmer, C. Smith, B. Fox-Kemper, H.T. Hewitt, C. Xiao, G. Aðalgeirsdóttir, S.S. Drijfhout, T.L. Edwards, N.R. Golledge, M. Hemer, G. Krinner, A. Mix, …, B. Pearson. 2021. IPCC AR6 Sea-level Rise Projections Version 20210809. https://podaac.jpl.nasa.gov/announcements/2021-08-09-Sea-level-projections-from-the-IPCC-6th-Assessment-Report.

Gattuso, J.-P., A. Magnan, R. Billé, W.W.L. Cheung, E.L. Howes, F. Joos, D. Allemand, L. Bopp, S.R. Cooley, C.M. Eakin, O. Hoegh-Guldberg, R.P. Kelly, H.-O. Pörtner, A.D. Rogers, J.M. Baxter, D. Laffoley, D. Osborn, A. Rankovic, J. Rochette, ..., C. Turley. 2015. Contrasting futures for ocean and society from different anthropogenic CO 2 emissions scenarios. *Science* 349 (aac6243): 4722. https://doi.org/10.1126/science.aac4722.

Gauthey, A., D. Backes, J. Balland, I. Alam, D.T. Maher, L.A. Cernusak, N.C. Duke, B.E. Medlyn, D.T. Tissue, and B. Choat. 2022. The role of hydraulic failure in a massive mangrove die-off event. *Frontiers in Plant Science* 13: 822136. https://doi.org/10.3389/fpls.2022.822136.

Hladik, C., and M. Alber. 2012. Accuracy assessment and correction of a LIDAR-derived salt marsh digital elevation model. *Remote Sensing of Environment* 121: 224–235. https://doi.org/10.1016/j.rse.2012.01.018.

Jia, M., Z. Wang, Y. Zhang, D. Mao, and C. Wang. 2018. Monitoring loss and recovery of mangrove forests during 42 years: The achievements of mangrove conservation in China. *International Journal of Applied Earth Observation and Geoinformation* 73: 535–545. https://doi.org/10.1016/j.jag.2018.07.025.

Jiang, J., D.L. DeAngelis, T.J. Smith, S.Y. Teh, and H.L. Koh. 2012. Spatial pattern formation of coastal vegetation in response to external gradients and positive feedbacks affecting soil porewater salinity: A model study. *Landscape Ecology* 27 (1): 109–119. https://doi.org/10.1007/s10980-011-9689-9.

Kirwan, M.L., and K.B. Gedan. 2019. Sea-level driven land conversion and the formation of ghost forests. *Nature Climate Change* 9 (6): 450–457. https://doi.org/10.1038/s41558-019-0488-7.

Kirwan, M.L., S. Temmerman, E.E. Skeehan, G.R. Guntenspergen, and S. Fagherazzi. 2016. Overestimation of marsh vulnerability to sea level rise. *Nature Climate Change* 6 (3): 253–260. https://doi.org/10.1038/nclimate2909.

Kirwan, M.L., G.R. Guntenspergen, A. D'Alpaos, J.T. Morris, S.M. Mudd, and S. Temmerman. 2010. Limits on the adaptability of coastal marshes to rising sea level. *Geophysical Research Letters*. https://doi.org/10.1029/2010GL045489.

Komiyama, A., J.E. Ong, and S. Poungparn. 2008. Allometry, biomass, and productivity of mangrove forests: A review. *Aquatic Botany* 89 (2): 128–137. https://doi.org/10.1016/j.aquabot.2007.12.006.

Kopp, R.E., R.M. Horton, C.M. Little, J.X. Mitrovica, M. Oppenheimer, D.J. Rasmussen, B.H. Strauss, and C. Tebaldi. 2014. Probabilistic 21st and 22nd century sea-level projections at a global network of tide-gauge sites. *Earth's Future* 2 (8): 383–406. https://doi.org/10.1002/2014ef000239.

Krauss, K.W., T.W. Doyle, R.R. Twilley, V.H. Rivera-Monroy, and J.K. Sullivan. 2006. Evaluating the relative contributions of hydroperiod and soil fertility on growth of south Florida mangroves. *Hydrobiologia* 569 (1): 311–324. https://doi.org/10.1007/s10750-006-0139-7.

Krauss, K.W., P.J. Young, J.L. Chambers, T.W. Doyle, and R.R. Twilley. 2007. Sap flow characteristics of neotropical mangroves in flooded and drained soils. *Tree Physiology* 27 (5): 775–783. https://doi.org/10.1093/treephys/27.5.775.

Krauss, K.W., D.R. Cahoon, J.A. Allen, K.C. Ewel, J.C. Lynch, and N. Cormier. 2010. Surface elevation change and susceptibility of different mangrove zones to sea-level rise on Pacific high islands of Micronesia. *Ecosystems* 13 (1): 129–143. https://doi.org/10.1007/s10021-009-9307-8.

Krauss, K.W., A.S. From, T.W. Doyle, T.J. Doyle, and M.J. Barry. 2011. Sea-level rise and landscape change influence mangrove encroachment onto marsh in the Ten Thousand Islands region of Florida, USA. *Journal of Coastal Conservation* 15 (4): 629–638. https://doi.org/10.1007/s11852-011-0153-4.

Krauss, K.W., K.L. Mckee, C.E. Lovelock, D.R. Cahoon, N. Saintilan, R. Reef, and L. Chen. 2014. How mangrove forests adjust to rising sea level. *New Phytologist* 202 (1): 19–34. https://doi.org/10.1111/nph.12605.

Krauss, K.W., and J.A. Allen. 2003. Factors influencing the regeneration of the mangrove Bruguiera gymnorrhiza (L.) Lamk. On a tropical Pacific island. *Forest Ecology and Management* 176 (1): 49–60. https://doi.org/10.1016/S0378-1127(02)00219-0.

Lander, M., and S. Khosrowpanah. 2004. A rainfall climatology for Pohnpei Island, The Federated States of Micronesia. Water and Environmental Research Institute of the Western Pacific, University of Guam. Technical report 100, p. 51.

Langston, A.K., O. Durán Vinent, E.R. Herbert, and M.L. Kirwan. 2020. Modeling long-term salt marsh response to sea level rise in the sediment-deficient Plum Island Estuary. *MA. Limnology and Oceanography* 65 (9): 1–16. https://doi.org/10.1002/lno.11444.

Leong, R.C., D.A. Friess, B. Crase, W.K. Lee, and E.L. Webb. 2018. High-resolution pattern of mangrove species distribution is controlled by surface elevation. *Estuarine, Coastal and Shelf Science* 202: 185–192. https://doi.org/10.1016/j.ecss.2017.12.015.

Lewis, R.R., E.C. Milbrandt, B. Brown, K.W. Krauss, A.S. Rovai, J.W. Beever, and L.L. Flynn. 2016. Stress in mangrove forests: Early detection and preemptive rehabilitation are essential for future successful worldwide mangrove forest management. *Marine Pollution Bulletin* 109 (2): 764–771. https://doi.org/10.1016/j.marpolbul.2016.03.006.

López-Medellín, X., E. Ezcurra, C. González-Abraham, J. Hak, L.S. Santiago, and J.O. Sickman. 2011. Oceanographic anomalies and sea-level rise drive mangroves inland in the Pacific coast of Mexico. *Journal of Vegetation Science* 22 (1): 143–151. https://doi.org/10.1111/j.1654-1103.2010.01232.x.

Lovelock, C.E., D.R. Cahoon, D.A. Friess, G.R. Guntenspergen, K.W. Krauss, R. Reef, K. Rogers, M.L. Saunders, F. Sidik, A. Swales, N. Saintilan, L.X. Thuyen, and T. Triet. 2015. The vulnerability of Indo-Pacific mangrove forests to sea-level rise. *Nature* 526 (7574): 559–563. https://doi.org/10.1038/nature15538.

Lovelock, C.E., R. Reef, and M.C. Ball. 2017. Isotopic signatures of stem water reveal differences in water sources accessed by mangrove tree species. *Hydrobiologia* 803 (1): 133–145. https://doi.org/10.1007/s10750-017-3149-8.

MacKenzie, R.A., P.B. Foulk, J.V. Klump, K. Weckerly, J. Purbospito, D. Murdiyarso, D.C. Donato, and V.N. Nam. 2016. Sedimentation and belowground carbon accumulation rates in mangrove forests that differ in diversity and land use: A tale of two mangroves. *Wetlands Ecology and Management* 24 (2): 245–261. https://doi.org/10.1007/s11273-016-9481-3.

MacKenzie, R.A., M. Apwong, K.J. Buffington, and K.M. Thorne. 2024. Soil characteristics and accretion rates in mangrove forests across Pohnpei, Federated States of Micronesia: U.S. Geological Survey data release. https://doi.org/10.5066/P967Y9KB.

Marani, M., A. D'Alpaos, S. Lanzoni, L. Carniello, and A. Rinaldo. 2010. The importance of being coupled: Stable states and catastrophic shifts in tidal biomorphodynamics. *Journal of Geophysical Research* 115 (F4): F04004. https://doi.org/10.1029/2009JF001600.

Mitra, A. 2020. Mangroves: A natural ecosystem of cultural and religious convergence. In *Mangrove Forests in India: Exploring Ecosystem Services*, 337–352. Springer International Publishing.

Morris, J.T., P.V. Sundareshwar, C.T. Nietch, B. Kjerfve, and D.R. Cahoon. 2002. Responses of coastal wetlands to rising sea level. *Ecology* 83 (10): 2869–2877.

Morris, J.T., D.C. Barber, J.C. Callaway, R. Chambers, S.C. Hagen, C.S. Hopkinson, B.J. Johnson, P. Megonigal, S.C. Neubauer, T. Troxler, and C. Wigand. 2016. Contributions of organic and inorganic matter to sediment volume and accretion in tidal wetlands at steady state. *Earth's Future* 4 (4): 110–121. https://doi.org/10.1002/2015EF000334.

Morris, J.T., J.A. Langley, W.C. Vervaeke, N. Dix, I.C. Feller, P. Marcum, and S.K. Chapman. 2023. Mangrove trees outperform saltmarsh grasses in building elevation but collapse rapidly under high rates of sea-level rise. *Earth's Future* 11 (4): e2022EF003202. https://doi.org/10.1029/2022EF003202.

Mycoo, M., M. Wairiu, D. Campbell, V. Duvat, Y. Golbuu, S. Maharaj, J. Nalau, P. Nunn, J. Pinnegar, and O. Warrick. 2022. Small Islands. In *Climate change 2022: Impacts, adaptation and vulnerability. Contribution of Working Group II to the Sixth Assessment Report of the Intergovernmental Panel on Climate Change*, ed. H.-O. Pörtner, D.C. Roberts, M. Tignor, E.S. Poloczanska, K. Mintenbeck, A. Alegría, M. Craig, S. Langsdorf, S. Löschke, V. Möller, A. Okem, and B. Rama, 2024–2121. Cambridge, UK and New York, NY, USA: Cambridge University Press. https://doi.org/10.1017/9781009325844.017.

Naylor, R.L., K.M. Bonine, K.C. Ewel, and E. Waguk. 2002. Migration, markets, and mangrove resource use on Kosrae, Federated States of Micronesia. *Ambio* 31 (4): 340:350.

Nunn, P.D., A. Kohler, and R. Kumar. 2017. Identifying and assessing evidence for recent shoreline change attributable to uncommonly rapid sea-level rise in Pohnpei, Federated States of Micronesia, Northwest Pacific Ocean. *Journal of Coastal Conservation* 21 (6): 719–730. https://doi.org/10.1007/s11852-017-0531-7.

Osland, M.J., L.C. Feher, J. López-Portillo, R.H. Day, D.O. Suman, J.M. Guzmán Menéndez, and V.H. Rivera-Monroy. 2018. Mangrove forests in a rapidly changing world: Global change impacts and conservation opportunities along the Gulf of Mexico coast. *Estuarine, Coastal and Shelf Science* 214: 120–140. https://doi.org/10.1016/j.ecss.2018.09.006.

Phan, S.M., H.T.T. Nguyen, T.K. Nguyen, and C. Lovelock. 2019. Modelling above ground biomass accumulation of mangrove plantations in Vietnam. *Forest Ecology and Management* 432: 376–386. https://doi.org/10.1016/j.foreco.2018.09.028.

Raabe, E.A., L.C. Roy, and C.C. McIvor. 2012. Tampa Bay coastal wetlands: Nineteenth to twentieth century tidal marsh-to-mangrove conversion. *Estuaries and Coasts* 35 (5): 1145–1162. https://doi.org/10.1007/s12237-012-9503-1.

Raynor, W.C., and J.H. Fownes. 1991. Indigenous agroforestry of Pohnpei. *Agroforestry Systems* 16 (2): 139–157. https://doi.org/10.1007/BF00129745.

Reef, R., M. Slot, U. Motro, M. Motro, Y. Motro, M.F. Adame, M. Garcia, J. Aranda, C.E. Lovelock, and K. Winter. 2016. The effects of CO_2 and nutrient fertilisation on the growth and temperature response of the mangrove Avicennia germinans. *Photosynthesis Research* 129 (2): 159–170. https://doi.org/10.1007/s11120-016-0278-2.

Rodríguez-Rodríguez, J.A., J.E. Mancera-Pineda, and H. Tavera. 2021. Mangrove restoration in Colombia: Trends and lessons learned. *Forest Ecology and Management* 496: 119414. https://doi.org/10.1016/j.foreco.2021.119414.

Rogers, K. 2021. Accommodation space as a framework for assessing the response of mangroves to relative sea-level rise. *Singapore Journal of Tropical Geography* 42 (2): 163–183. https://doi.org/10.1111/sjtg.12357.

Rybczyk, J.M., J.C. Callaway, and J.W. Day Jr. 1998. A relative elevation model for a subsiding coastal forested wetland receiving wastewater effluent. *Ecological Modelling* 112 (1): 23–44. https://doi.org/10.1016/S0304-3800(98)00125-2.

Saintilan, N., N.S. Khan, E. Ashe, J.J. Kelleway, K. Rogers, C.D. Woodroffe, and B.P. Horton. 2020. Thresholds of mangrove survival under rapid sea level rise. *Science* 368 (6495): 1118–1121. https://doi.org/10.1126/science.aba2656.

Sherman, R.E., T.J. Fahey, and P. Martinez. 2003. Spatial patterns of biomass and aboveground net primary productivity in a mangrove ecosystem in the Dominican Republic. *Ecosystems* 6 (4): 384–398.

Sierra-Correa, P.C., and J.R. Cantera Kintz. 2015. Ecosystem-based adaptation for improving coastal planning for sea-level rise: A systematic review for mangrove coasts. *Marine Policy* 51: 385–393. https://doi.org/10.1016/j.marpol.2014.09.013.

Spencer, T., M. Schuerch, R.J. Nicholls, J. Hinkel, D. Lincke, A.T. Vafeidis, R. Reef, L. McFadden, and S. Brown. 2016. Global coastal wetland change under sea-level rise and related stresses: The DIVA Wetland Change Model. *Global and Planetary Change* 139: 15–30. https://doi.org/10.1016/j.gloplacha.2015.12.018.

Swanson, K.M., J.Z. Drexler, D.H. Schoellhamer, K.M. Thorne, M.L. Casazza, C.T. Overton, J.C. Callaway, and J.Y. Takekawa. 2014. Wetland accretion rate model of ecosystem resilience (WARMER) and its application to habitat sustainability for endangered species in the San Francisco estuary. *Estuaries and Coasts* 37 (2): 476–492. https://doi.org/10.1007/s12237-013-9694-0.

Thorne, K., G. MacDonald, G. Guntenspergen, R. Ambrose, K. Buffington, B. Dugger, C. Freeman, C. Janousek, L. Brown, J. Rosencranz, J. Holmquist, J. Smol, K. Hargan, and J. Takekawa. 2018. U.S. Pacific coastal wetland resilience and vulnerability to sea-level rise. *Science Advances*. https://doi.org/10.1126/sciadv.aao3270.

van Maanen, B., G. Coco, and K.R. Bryan. 2015. On the ecogeomorphological feedbacks that control tidal channel network evolution in a sandy mangrove setting. *Proceedings of the Royal Society a: Mathematical, Physical and Engineering Science* 471 (2180): 20150115. https://doi.org/10.1098/rspa.2015.0115.

Watson, J.G. 1928. Mangrove forests of the Malay Peninsula. *Malayan Forest Records* 6: 1–275.

Widlansky, M.J., A. Timmermann, K. Stein, S. McGregor, N. Schneider, M.H. England, M. Lengaigne, and W. Cai. 2013. Changes in South Pacific rainfall bands in a warming climate. *Nature Climate Change* 3 (4): 417–423. https://doi.org/10.1038/nclimate1726.

Williams, K., K.C. Ewel, R.P. Stumpf, F.E. Putz, and T.W. Workman. 1999. Sea-level rise and coastal forest retreat on the west coast of Florida, USA. *Ecology* 80 (6): 2045–2063. https://doi.org/10.1890/0012-9658(1999)080[2045:SLRACF]2.0.CO;2.

Woltz, V.L., E.I. Peneva-reed, Z. Zhu, E.L. Bullock, R.A. MacKenzie, M. Apwong, K.W. Krauss, and D.B. Gesch. 2022. A comprehensive assessment of mangrove species and carbon stock on Pohnpei. Micronesia. *PLoS One* 17 (7): e0271589. https://doi.org/10.1371/journal.pone.0271589.